Springer

Chinese Society of Pavement Engineering

International Journal of
Pavement Research and Technology

Journal homepage: www.springer.com/42947

Optimization of electric arc furnace aggregates replacement in dense-graded asphalt wearing courses

Federico Autelitano*, Felice Giuliani

Department of Engineering and Architecture, University of Parma, Parco Area delle Scienze, 181/A - 43124 Parma, Italy

Received 10 April 2020; received in revised form 7 August 2020; accepted 17 August 2020; available online 2 September 2020

Abstract

Electric arc furnace (EAF) aggregates, by-products of the homonymous steelmaking process, represent an ideal solution for asphalt mixtures, above all for wearing courses where skid resistance and durability are essential functional requirements. Their use, which is subordinate to the compliance of chemical specifications, finds some practical interest limits mainly related to transportation (extremely high bulk specific gravity) and placement (unsatisfactory compaction) operations. Thus, the aim of this experimental study was to determine an ideal artificial to natural aggregates replacement rate, also identifying the most suitable particle size range, for dense-graded asphalt wearing courses. The results highlighted how the best balance between compaction and mechanical performances was registered by a mix which was formulated considering a partial replacement of 54% (v/v%), distributed only in the coarsest fraction. The introduction of limestone as "excipient" in the coarse-fine and finer size ranges reduces the weight of the mixture, guaranteeing at the same time an optimum compaction degree, high levels of stiffness in the viscous-elastic region and Marshall stability and extended fatigue life.

Keywords: Steel slag; Industrial by-product; Recycled material; Hot mix asphalt; Pavement engineering; Compaction

1. Introduction

The future of construction, and in particular of road construction, unavoidably passes through the paradigm of the circular economy and the application of strategies aimed at reducing the impact of interventions and pushing the recycling of materials [1]. In this perspective, many countries have developed policies for limiting the materials extracted from quarries and enhancing the re-use of reclaimed asphalt pavement (RAP) or the recycling of industrial wastes and by-products that otherwise would be send to landfills for disposal [2-5]. Thus, several in-place or in-plant recycling techniques for old asphalt pavements, based on hot and cold procedures, have become established over the years [6-10]. Besides, many cross-sectoral projects have seen the development of symbiotic collaboration with industries for the implementation of innovative technological processes able to transform waste into valuable and cost-effective construction materials [11,12].

In this "end of waste" context, a preferential partner and stakeholder for the road construction sector has been the steel industry, which needed to optimize the combination of competitiveness and sustainability by pursuing the zero-waste model. Steel industry represents a strategic division and a key element for the economy of many industrialized countries. Just think that the world crude steel production in 2019 was about 1.8 billion tons, mainly attributed to the basic oxygen furnace (BOF) and electric arc furnace (EAF) production techniques [13]. The latter represents one of the emblematic sector of sustainable industry. The raw materials of EAF steelmakers are steel scraps of different sources, which return upstream of the production chain following a theoretically infinite cyclic path. Roughly 29% of the total worldwide crude steel came from EAF mills, with peaks of 60-70% in several countries of European Union, NAFTA, Africa and Middle East. As the world's biggest steel producer (928 million tons), the Chinese situation has a significant impact on the global statistics. China's steel scrap consumption dropped around 4.8% in 2015, but over the past two years there has been a renewed interest in the usage of electric-arc furnaces (up to 12%), which are increasingly replacing the basic-oxygen furnaces. EAF steelmaking is to date nearing zero-waste, with current material efficiency rates near to 100%, i.e. over 96% of raw materials used on-site are converted to products and wastes or by-products are used or recycled [13,14]

The slags produced during the EAF metallurgical process are directed towards a secondary chain aimed at transforming them into marketed products, which are certified as artificial aggregates. Specifically, slags derived from the combination during the

* Corresponding author
E-mail address: federico.autelitano@unipr.it; https://orcid.org/0000-0003-0780-9438 (F. Autelitano); felice.giuliani@unipr.it; http://orcid.org/0000-0002-8842-5083 (F. Giuliani).
Peer review under responsibility of Chinese Society of Pavement Engineering.

ISSN: 1997-1400 DOI: https://doi.org/10.1007/s42947-020-0099-8

melting process of non-metallic scrap components and steel incompatible elements with fluxes, in the form of burnt lime or dolomite. After the liquid slags are poured, they undergo a multi-stage process which involves a controlled cooling, a primary crushing of the solidified material, a magnetic metal recovery step followed by sizing and screening [15,16]. Finally, steel slags are stockpiled separately according to their particle size ranges and stabilized/aged for several weeks (exposure to weathering, use of additives, water quenching or spaying, high temperature steam treatment) to promote the hydration and carbonation of expansive compounds (free CaO and MgO), which could otherwise generate the aggregates volume instability [17,18]. In general, this type of artificial aggregate can be assimilated to volcanic igneous rocks and mainly consists of a ternary mixture of calcium oxide (CaO), silicon dioxide (SiO_2) and iron oxides (FeO), together with minor components which include the remaining oxidized impurities present in the hot metal [19]. However, the mineralogical composition, as well as the structure, the chemical-physical and mechanical properties are strongly influenced and depend on the characteristics of the raw materials, the adopted technologies and the molten slag treatments [20] Steelmakers have exploited in recent years the potential of the best available techniques (BAT) to enhance the quality of their slags, which today are in most cases considered environmentally sound as natural primary products and do not present any increased risk to human health or the environment. However, the valorization of these by-products is regulated by national and international directives, which identify specific technical protocols (e.g. European Union CE marking) able to certify the slags chemical inertia and the absence or the very limited presence of potential toxic trace of metalloids (including Al, Cr, Pb, Mo and V) mobilized in the alkaline leachate [21,22].

Numerous studies and full-scale works have highlighted the total suitability, from a technical point of view, of these materials for several civil engineering purposes, such as cement production, concrete aggregates and soil stabilization, but the most common application was in road construction sectors [23-26]. EAF aggregates are typically used in asphalt layers, cement-treated load-bearing layers or unbound road bases or sub-bases [17,27-29]. A very high degree of roughness, surface irregularities or sharp angles on the one hand and an excellent toughness, hardness, abrasion and polishing resistance on the other associated to a very good affinity to asphalt binder, make EAF aggregates an ideal solution for asphalt mixtures, above all for wearing courses where of skid resistance and durability to high traffic- and environmentally-induced stresses are essential functional requirements [30,31]. Asphalt layers containing steel aggregates show excellent and improved engineering properties, such as Marshall stability, indirect tensile strength, dynamic and resilient modulus (stiffness), fatigue and resistance to permanent deformation [32-36]. Besides, given the enhanced thermal properties and fire behavior, these mixtures turn out to be an attractive solution for asphalt pavements in tunnels [37]. These satisfactory performances have been proven for traditional hot mix asphalt (HMA), asphalt mixtures containing also RAP and prepared exploiting the warm mix asphalt (WMA) technology [38-40]. Although there is an established evidence about the excellent potential of using these artificial aggregates in asphalt layers, the ideal amount of replacement and the correct particle size range are still debated topics. Asphalt mixes entirely made of EAF aggregates could show some drawbacks mainly related to transportation and placement. The extremely high bulk specific gravity (about 3700-3900 kg/m^3) of the EAF aggregates, due to the presence of iron oxides, produces heavyweight mixtures which could lead to variations in transportation planning, with a consequent increase in overall costs, fuel consumption and the necessity of more trucks to provide a given delivery rate (expressed in m^3/h). Besides, the rough surface texture of steel aggregates could represent to some extent a practical limit: the generation of high levels of friction between aggregate particles and the mixture negatively affect the compactability of the mixture, which results to be too rich in air voids and more prone to moisture damage and rapid age hardening [29]. Several studies stated that the best results were obtained considering a partial replacement of natural by EAF aggregates quantifiable in around 30%, but many others highlighted how a higher artificial aggregates content could lead to asphalt mixtures characterized by excellent mechanical and physical behavior, meeting multiple performance requirements [41-44]. In terms of size range, most authors agree that only coarser steel aggregates should be considered, although others argue that also fine grain size can also be used [45-47].

Hence, the aim of this experimental study was to provide an additional contribution to the analysis of the influence of EAF aggregates on the compaction and engineering properties of HMA for wearing course to define an ideal natural aggregate replacement rate. Besides the quantitative aspect, the identification of the most suitable particle size range would make it possible to enhance the positive contribution of artificial steel aggregates in asphalt pavements, not considering their use only a recycling strategy. The whole mix design process, based on a correct integration of EAF aggregates in the gradation curve, should not only be thought to improve the mixtures' expected performances but also to provide a tool for technical-economic analyses on the convenience of using them according to transport practices from a production facility to a paving site and the related application techniques. For this purpose, some asphalt mixtures characterized by different contents of artificial aggregates blended with limestone, as partial replacement in the coarse and coarse-fine fraction, have been designed and tested for a rank comparison, which represented the starting point for a critical reading key of the different highlighted behaviors.

2. Materials characterization

Two different kinds of aggregates were selected for the experimental analysis: limestone and certified EAF aggregates. Specifically, these EAF aggregates derived from steel slags produced during the metallurgical process of electric furnace smelting of ferrous and cast iron scraps. Slags were cooled and treated (iron removal) and then subjected to crushing, screening and aging (open-air stockpiling for more than 6 months). These production and treatment cycles have generated a by-product whose major chemical components were FeO (38-40%), SiO_2 (18-19%), CaO (16-18%), Al_2O_3 (5-6%), MnO (2.5-3%) and MgO (2-2.5%), which together represent more than the 80% of the total mass. The large iron oxides content leads to heavyweight and dark particles. Thus, the artificial aggregates showed high bulk specific gravity (3825-3983 kg/m^3), with increasing values as the particles size decrease, larger than that of limestone (2753 kg/m^3). They were dark grey and totally crushed or broken particles characterized by a suitable form and angularity associated with porous and rough surface. EAF aggregates showed a quite low vulnerability to freeze-thaw degradation and water absorption degree. A good porosity level and suitable surface characteristics, in addition to ensure a proper aggregate-asphalt binder interaction,

increase the pavement friction or skid resistance. Besides, mechanical tests highlighted excellent toughness, hardness, abrasion and polishing resistance, which were testified by very low Los Angeles and micro-Deval abrasion number and high Polished Stone Value. These properties positively affect the stability and fatigue resistance of HMA mixtures. The physical and mechanical characterization of EAF and limestone aggregates is summarized in Table 1.

Dense-graded asphalt wearing courses were prepared using a neat virgin 50/70 penetration grade asphalt cement. The aggregate/binder affinity (stripping) was preliminarily assessed through a boiling test. The procedure measured the moisture susceptibility to the binder adhesion by evaluating the amount of asphalt cement that remains after boiling in distilled water for 30 min on a sample of asphalt mixture (12.50/19.00 mm fraction; 5% volume binder content). The amount of stripping was expressed in terms of the percent of asphalt retained, as mean value of three independent samples. No significant difference emerged in the asphalt retained by EAF (51.55%) and limestone aggregates (52.08%).

3. Methods

Four different HMA wearing course mixtures, each containing different contents of natural and artificial aggregates, were analyzed. The aggregate fractions were combined considering the grading curve reported in Table 2, which is in accordance to the dense-coarse gradation reported in the international standards and specifications for wearing courses.

One mix (S-100) was prepared only with EAF aggregates, whereas two mix types were designed using steel aggregates as partial replacement in the coarse and coarse-fine fraction: the S-70 was composed of 67.5% (v/v %) EAF aggregates (2.36/19.00 mm) and 32.5% limestone (0/2.36 mm), whereas the S-50 mixture of 54.0% (v/v%) EAF aggregates (4.75/12.50 mm) and 46.0% limestone (0/4.75 mm). A reference mix was entirely made up of natural limestone aggregates (L). A limestone filler was used in all mixtures. The blending of aggregates with different mineralogical nature and bulk specific gravity required a volumetric approach in the mix design. Aggregates homogenization coefficients, defined as ratio between the specific gravity of the i-th size range and the mean value of the *j*-th mix (c_{ij} = $G_{i\text{-size range}}/G_{j\text{-mixture}}$), were introduced to convert the volume to weight values, which were obtained multiplying the volume values by the c_{ij} factors. An asphalt cement volume nominal content of 5.5 % was considered to prepare the HMA mixtures. This binder content has been selected downstream of a preliminary Marshall mix design procedure: all blends showed the best balance between density, air voids and Marshall quotient (ratio between stability and flow), unless small differences quantifiable in two or three tenths of a percentage point at most, right near the 5.5%. In the light of these data and to avoid the introduction of an additional variable, i.e. the asphalt binder content, to the experimental matrix, the use of same quantity of nominal binder in volume was deemed more appropriate. Then, asphalt homogenization coefficients, defined as the ratio between densities of the *j*-th and L mix, were identified to calculate the correct weight content for each mixture.

The experimental procedure was divided into two sequential operational steps. The first phase, which was conducted on all the four mixtures, was aimed at identifying, through a mechanical and volumetric approach, the influence of EAF aggregates on the compaction properties and stiffness of HMA. Once the most performing EAF-based mixture had been identified, it was the subject of an additional investigation, together with the reference mixture, to determine various engineering properties.

3.1. Step 1: Compaction properties and stiffness determination

The first phase involved the execution of the dynamic modulus test, according to a modified ASTM D3497 [48] procedure, on samples prepared with the SuperPave gyratory compactor (Pine Instrument Company). Preheated aggregates and asphalt cement were mixed at 160-170°C and then compacted applying a constant vertical pressure of 600 kPa while rotating for 100 gyrations (rate of 30 rpm) with an eccentricity of 1.25° from the vertical axis. Cylindrical samples with a diameter (*D*) of 100 mm and a nominal thickness (*t*) of 125 mm were prepared. The specimens were stored on a flat surface at laboratory conditions (T = 22 ± 2°C; RH = 55 %) for 14 days from the time of their manufacture and preconditioned prior to the start of testing, in a thermostatically controlled air chamber, to the selected temperature for 2 h.

Table 1
Physical and durability properties of EAF and limestone aggregates.

Test	Symbol	Unit	EAF 0/4.75 mm	EAF 4.75/9.5 mm	EAF 9.5/19 mm	Limestone 0/19 mm
Fines content	*f*	%	1.4	1.3	1.3	1.8
Sand equivalent	*SE*	%	84	-	-	69
Flakiness index	*FI*	%	-	13.1	11.6	10.8
Shape index	*SI*	%	-	7.7	7.6	7.0
Los Angeles coefficient (%)	*LA*	%	-	13.0	12.4	23.1
Micro-Deval coefficient (%)	M_{DE}	%	-	6.8	6.5	13.5
Polished stone value (%)	*PSV*	%	-	54.3	62.1	47.9
Water absorption (%)	*WA*	%	0.7	0.6	0.6	0.5
Freezing and thawing resistance	*F*	%	2.1	1.9	1.8	1.2
Bulk specific gravity	G_B	kg/m^3	3983	3903	3825	2753

Table 2
Selected grading curve for the HMA wearing course.

Sieve (mm)	19.00	12.50	9.50	4.75	2.36	0.30	0.15	0.075
Cumulative passing (%)	100	89	78	46	33.5	15	11	8

A repeated axial cyclic load test was performed to determine the HMA stress-strain relationship. Tests were carried out using the servo hydraulic MTS 810 (Material Testing System Corporation) system, which was equipped with a 25 kN electronic load cell and an environmental chamber. Specimens were instrumented with extensometers to measure the material deformation. Specifically, the complex modulus (E^*), which represent the ratio between the applied stress ($\sigma = \sigma_0 \cdot sen(\omega t)$) and the measured strain ($\varepsilon = \varepsilon_0 \cdot sen(\omega t - \phi)$) that has a phase angle ϕ with respect to the stress, was determined. Tests were performed on stress-controlled loading mode applying a dynamic sinusoidal (haversine) axial compressive stress to the cylindrical specimen at four temperatures (0, 10, 25, and 40°C) and at six loading frequencies (0.1, 0.5, 1, 5, 10 and 25 Hz) for each temperature. The testing sequence started with the highest frequency and moved to the lowest in ascending order of temperature. A loading period of 30 s and a rest period between any two consecutive loading frequencies of 120 s were assigned. A conditioning period of 2 hours was assumed for adjusting the sample temperature when proceeding from one temperature to the next. Three specimens for each of the four mixtures were prepared and tested.

Before conducting the performance test, the theoretical maximum specific gravity (G_{mm}) of the uncompact mixtures and the bulk specific gravity (G_{mb}) of the extruded specimens, were determined according to the ASTM D 2041 and ASTM D2726 specifications [49,50]. With the knowledge of these two parameters and exploiting the potential of the gyratory compactor to real-time monitor the change in specimen height, the asphalt mixture compaction and volumetric properties were back-calculated for any number of gyrations and analyzed. Continuous densification curves, which display the increase in specimen density (expressed as $\%G_{mm}$) with increasing compactive effort (number of gyrations N_g), were plotted and the compaction energy index (*CEI*) and the compaction slope (k) were introduced. *CEI*, which represents the work applied by the roller to compact the mixture to the required density during construction, is calculated as the area from the 8th gyration (paver effort applied during laying down the mixture) to 92% of G_{mm} (pavement open to traffic density) in the densification curve as shown in Fig. 1 [51]. Adopting a logarithmic scale on the horizontal axis, the densification curve assumes an almost straight trend, which is well described using a linear interpolation:

$$\%G_{mm} = C_1 + k \cdot Log(N_g) \quad (1)$$

where, C_1 defines the self-compaction, that identifies the compaction degree at the first gyration (initial vertical shift factor), whereas k represents the compaction slope of the regression line and explain the mixture workability. The interpolation was evaluated between the 8th and the 100th gyration, as suggested by SuperPave recommendations.

3.2. Step 2: In-depth analysis of the optimized EAF mixture

Once identified the optimum EAF aggregates replacement, the selected mixture was studied to measure some salient parameters of wearing course, i.e. Marshall quantities (stability - *MS* and flow - *MF*) and indirect tensile strength (S_t). The Marshall compression tester (Controls Group) and the servo hydraulic MTS 810 (Material Testing System Corporation) system and the were used to determine the Marshall parameters the S_t, respectively. Tests were performed on samples prepared with the SuperPave gyratory compactor using the same compaction parameters (vertical

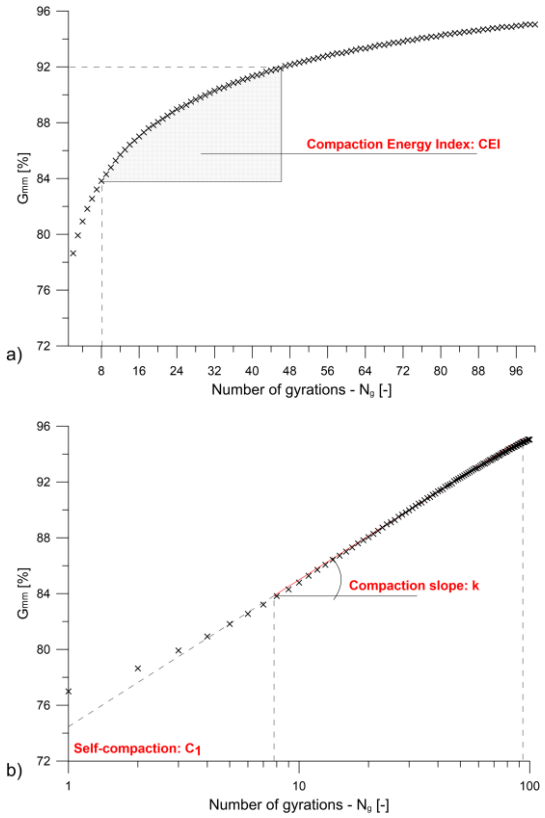

Fig. 1. Densification curve for the determination of densification index: (a) *CEI* and (b) k.

pressure: 600 kPa; gyrations: 100; eccentricity: 1.25°) and stored before testing following the same procedure (14 days at laboratory condition). Cylinder shaped specimens with a diameter (D) of 100 mm and a nominal thickness (t) of 63.5 mm were considered and tested. A total of 48 (24 for each mixture) specimens were prepared, i.e. 3 for each test configuration.

Marshall stability-flow test (ASTM D6927) [52] was used to measure the resistance to plastic flow of HMA specimens loaded at 60°C with a constant rate of deformation (50.8 mm/min) in a direction perpendicular to the cylindrical axis. Marshall stability (*MS*) is the peak resistance load obtained during the loading sequence, whereas flow (*MF*) is the maximum vertical deformation at the failure point. The Marshall stability values were then compared with those of a second subset of samples, which underwent a water conditioning, to evaluate the mixture moisture sensitivity. Specifically, the second subset was preliminary conditioned by vacuum saturating with distilled water to 70-80% of the air void volume and subsequent soaking in a 60°C water bath for 72h. The Marshall stability ratio ($MSR=MS_{wet}/MS_{dry}$), calculated as ratio between the average values of the dry and wet subsets, expressed the resistance to moisture induced damage as a ratio of the unconditioned sample *MS* that is retained after the conditioning. Besides, the specimens' volume was measured before and after the water immersion to monitor the potential expansion of EAF aggregates from hydration reactions.

The tensile characteristics of HMA mixtures were evaluated by loading, diametrically along the direction of the cylinder axis, the specimens with a continuous compressive load at a constant rate of deformation of 50.8 mm/min, according to ASTM D6931 [53], until breaking at 25°C. The indirect tensile strength (S_t) is the maximum tensile stress calculated from the peak load applied at

break (P) and the dimensions of the specimen, according to the equation:

$$S_t = \frac{2P}{\pi \cdot t \cdot D} \quad (2)$$

Using the indirect tensile test (IDT) configuration, samples were also subjected to the indirect tensile fatigue test (ITFT) to characterize their fatigue life at intermediate pavement operating temperatures [54,55]. Specimens were exposed at 15°C to repeated compressive loads, through the vertical diametrical plane, with a haversine cyclic force signal without any rest periods at a frequency of 10 Hz. The specimens were tested at five load levels, referable to about the 20, 25, 35, 45 and 55% of the peak load at break (P) registered in the IDT. Permanent vertical deformation and transient vertical deformation (Δ_p) were measured with linear variable differential transformers (LVDT's). The maximum horizontal tensile stress at the center of the specimen ($\sigma_{x,max}$) was determined using a relationship similar to Eq. (2), where P is in this case the applied vertical force. Fatigue life was then defined on the basis of the dissipated energy approach [56]. Thus, fatige life was cosidered the number of cycles up to the point of crack initiation (N_1), which was identified in correspondance of the peak of the curve described by the number of cycles (N_c) divided by the transient vertical deformation (Δ_p) against the number of cycles (N_c) (Fig. 2).

4. Results

4.1. Step 1: Optimum EAF aggregates replacement rate identification

Starting from the physical parameters obtained from the tests carried out on aggregates, loose and compacted mixtures, the

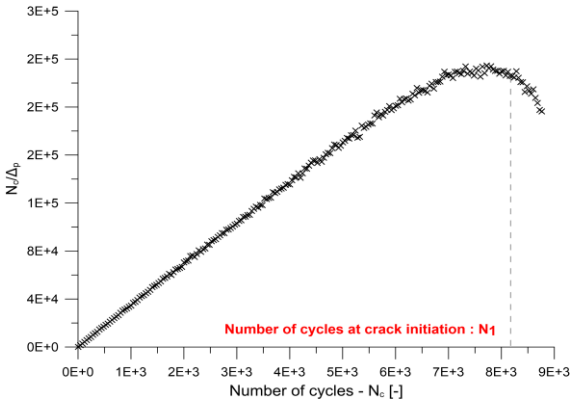

Fig. 2. Graphical definition of the point of crack initiation (N_1).

volumetric properties of the compacted samples were back-calculated for any number of gyrations. Several parameters of the analyzed mixtures at 100 number of gyrations are summarized in Table 3. These data provide an interesting overview about the influence of EAF aggregates on the mixtures volumetric composition. Firstly, the S-50 mixture represented a rather ideal mix characterized by values close to those generally required in the HMA laboratory mix design criteria for medium and high level of traffic, which can be traced back to *VFA* values between 65 and 78%, *VMA* greater than 14% and *VA* of approximately 4%. Mixtures containing higher EAF aggregates content showed greater *VMA* and excessive *VA* (8-10%), which could make the pavement too permeable to air and water, resulting in significant moisture damage and rapid age hardening. This behavior, which was registered by other researchers [29,32,42], is mainly attributable to the rougher texture of EAF aggregates, which generating more friction between aggregate particles and the mixture increased the compaction resistance. Hence, for a given number of gyrations, the mixture did not compact as much. Instead, the reference limestone mix resulted to be ultra-compacted (*VA* = 2.2%). Also this condition should also be avoided since it could be predictive of a mixture more prone to rutting. Thus, the replacement of EAF aggregates only in the coarser fraction (5-15 mm) produce denser (< *VA*) and lighter (< G_{mm}) mixtures, which inevitably translate into better pavement performances and economic and practical benefits during the HMA transport from the production facility to the paving site.

The difficulty of compaction registered for S-70 and S-100 mixture is very clearly also found when examining the densification data (Table 4). In energetic terms, the S-50 mixture represented the best one presenting values within the range delimited by minimum values that characterize too tender mixtures and maximum values that describe mixtures with unacceptable compactability. The *CEI* calculated for the S mixture have been defined using the greater-than sign since a $\%G_{mm}$ level equal to 92% has not been reached even at the 100th gyration. As regards the compaction slope, which is considered a workability indicator, there was an increase in k and C_1 parameters with a reduction in the EAF content. Specifically, the S-50 and L densification curve were almost parallel and only slightly vertical shifted due to the little difference in the self-compaction at 1st gyration (Fig. 3).

The proposed mechanical characterization of HMA containing EAF aggregates, was based on the performance test used to measure the complex modulus, which represent a stiffness parameter. At initial analysis, the influence of frequency (traffic-related variable) and temperature (environment variable) on the asphalt materials' stiffness was evaluated. As expected, the complex modulus increased with the increase in loading frequency and decreased with increasing temperature, regardless the

Table 3
Volumetric properties of the analyzed HMA mixtures.

Volumetric parameter	Symbol	Unit	Mixture			
			S-100	S-70	S-50	L
Total asphalt binder content	P_b	w/w%	3.98	4.31	4.55	5.50
Overall bulk specific gravity for aggregate blend	G_{sb}	g/cm^3	3.804	3.515	3.331	2.753
Theoretical maximum specific gravity of loose mixture	G_{mm}	g/cm^3	3.547	3.253	3.045	2.466
Mixture bulk specific gravity	G_{mb}	g/cm^3	3.171	3.001	2.898	2.411
Air void content	*VA*	v/v%	10.60	7.75	4.84	2.22
Voids in the mineral aggregate	*VMA*	v/v%	19.96	18.22	16.97	17.23
Voids filled with asphalt	*VFA*	v/v%	46.92	57.48	71.48	87.14

Table 4
Densification parameters of the analyzed HMA mixtures.

Densification parameter	Mixture			
	S-100	S-70	S-50	L
$\%G_{mm}@N_{g8}$	81.00	85.03	87.92	86.44
$\%G_{mm}@N_{g100}$	89.40	92.25	95.16	97.78
$N_g@92\%G_{mm}$	> 100	93	45	25
k	3.73	3.87	4.32	4.55
C_1	72.24	73.97	75.45	77.24
CEI	> 632.04	594.69	187.88	63.71

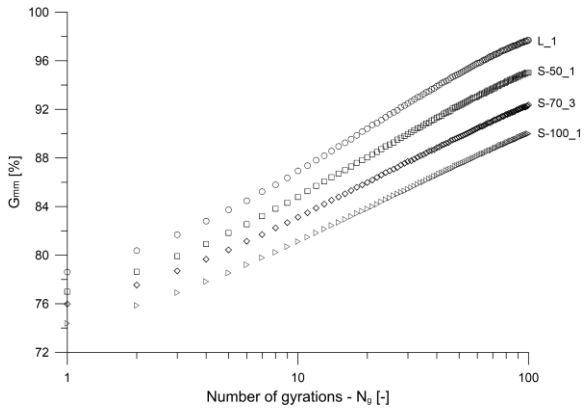

Fig. 3. Densification curves in a semi-Log plane.

aggregates mix. As far as the sensitivity of the complex modulus to the properties of the mix components is concerned, the difference between the HMA mixtures was evident across the whole frequency sweep at all four test temperatures. The isothermal curves reported in Fig. 4 highlight how the E^* values of the S-100 and S-70 mixtures were lower than those registered by the reference one, unlike the S-50 mix which turned out to be much stiffer. Complex modulus values measured for the first two mixtures decreased as the EAF replacement, and consequently the air voids content, increased, except for the temperature of 40°C in which the trend tends to reverse. Analyzing in detail the data related to the frequency range 0.5-5 Hz, traceable to the typical speeds of road vehicles, a decrease of 19-23% (slightly lower at 40°C) and 5-15% were identified for S-100 and S-70, respectively: the use of EAF aggregates in sand and/or coarse-fine fraction led to a significant reduction of the mixtures' stiffness. The ideal volumetric properties of the S-50 mix, which includes EAF aggregates only in the coarsest fraction (4.75-19 mm), translated into higher levels of stiffness, especially for medium low (10°C) and warm temperatures (25 and 40°C), with a maximum increase compared to the reference mixture of more than 40% over the whole frequency spectrum at 40°C.

4.2. Step 2: Rank comparison between L and S-50 mix

In the light of the results acquired in the first step, the in-depth analysis was conducted on the S-50 mixture for a rank comparison with the reference one. Firstly, the Marshall test parameters were evaluated (Table 5). Flow was reported both using its absolute value in mm and the increments of 0.25 mm. The first of the two flow values was used, as standard practice of the European highway agencies, for the calculation of the Marshall Quotient (MQ), which can be used to give an indication of the mixture stiffness, given by the ratio between stability and flow. In line with

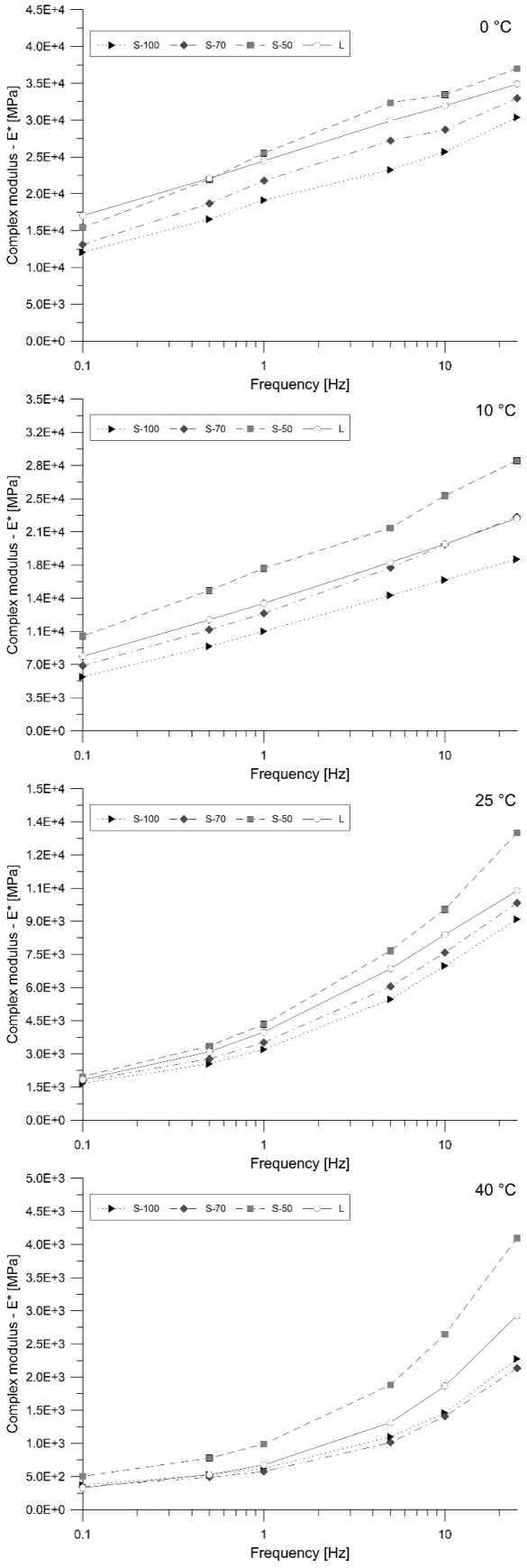

Fig. 4. Effect of EAF aggregates replacement on complex modulus evaluated in the frequency spectrum at different temperatures.

Table 5
Marshall and IDT parameters.

Parameter	Unit	Mixture	
		S-50	L
MS	kN	17.41	13.15
MF	mm	4.38	3.72
MF	0.25mm	17	14
MQ	kN/mm	4.05	3.63
MSR	-	0.86	0.92
S_t	MPa	1.00	1.01

the findings of other authors [29,33,36,45], the S-50 mixture combined a very high stability with good flow. The Marshall stability is controlled by the angle of internal friction of the aggregates, other than by the asphalt cement viscosity at the testing temperature. Thus, using more angular aggregates, such the EAF aggregates, higher Marshall stability were obtained. Moreover, the *MQ* values, confirmed the results of the complex modulus study, which described the S-50 as the stiffest mixture. Comparison of *MS* with that of the wet conditioned samples was used to assess the HMA moisture sensitivity. Firstly, no visual evidence of stripping in the conditioned test specimens was found in both mixtures. The Marshall ratio of the conditioned to unconditioned subset resulted to be greater than 80% and in analogy to the standardized procedure (ASTM D 4867) [57], which provides for IDT instead of Marshall stability test, both mixtures can be considered acceptable. The 87% of retained *MS* of the S-50 mix is an excellent target especially considering the very high values registered by the unconditioned samples. In addition, no significant changes in volume were recorded by the S-50 specimens stored in water, quantifiable in 0.2% which was comparable to that of the reference mixture. The very small volumetric variation was due both to the aging process to which the slags ware subjected after the crushing and screening phases that allowed the oxidation of the expansive compounds and to the containment effect produced by the asphalt binder film on the aggregates that inhibited their direct contact with water.

In parallel, IDT and ITFT were performed. The S_t values obtained for both mixtures were equal to about 1.00 MPa, which resulted from peak loads of about 10.65-10.80 kN. Starting from the IDT average peak load, five vertical loading values were considered for the fatigue test: 2.35, 3.05, 4.20, 5.35 and 6.40 kN. The addition of coarse EAF aggregates, as already highlighted in previous studies [33,35,41,42], improved the fatigue resistance: a higher fatigue life was exhibited by the S-50 mixture for all the load amplitudes. The graphical representation maximum horizontal tensile stress at the center of the specimen ($\sigma_{x,max}$) versus number of cycles at crack initiation (N_1) highlights how this difference remained almost constant (about 25%) over the whole stress spectrum (Fig. 5).

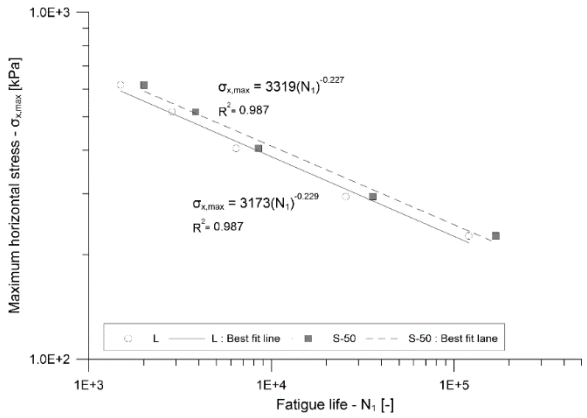

Fig. 5. Fatigue characteristics for L and S-50.

5. Conclusions

The experimental investigation on dense-graded wearing courses containing aggregates with excellent toughness, hardness, abrasion and polishing resistance, as the EAF aggregates are, provided an interesting overview about the influence of these industrial by-products on the mixtures engineering performances, also providing technical-economic food to overcome the known drawbacks related to the HMA transport and laying.

1. The use of EAF aggregates, which is subordinate to the certification of the materials' chemical inertia and the absence of potential toxic trace of metalloids in the leachate, finds a practical interest limit (transportation planning and related costs) due to their extremely high bulk specific gravity which produces heavyweight mixtures. The introduction of limestone as "excipient" in the coarse-fine and finer size ranges limits the theoretical maximum specific gravity of loose mixture while keeping unchanged the improved skid resistance and durability to high traffic-induced stresses, representing a smart approach to increase the commercial appeal of the EAF aggregate-based asphalt mixtures.
2. The choice to analyze mixtures consisted of fraction and mineral filler with very different bulk specific gravities required a volumetric approach, which relied on mixing constituent materials on the basis of their volume. Homogenization coefficients were introduced to convert the theoretic volume contents to the easier to measure weights.
3. Three mixes prepared with a blend of EAF and limestone aggregates and a reference one entirely made up of limestone were considered. Specifically, a total (S-100) and a partial replacement of coarse particle size range (S-70 and S-50) were selected.
4. The best balance between compaction and mechanical performances was registered by the S-50 mix, which was formulated considering a replacement rate of 54% (v/v%), distributed only in the coarsest fraction 4.75-19 mm. This mixture was characterized by an optimum compaction degree, testified by both volumetric (*VA*, *VMA*) and densification parameters (k, C_1 and *CEI*), high levels of stiffness (E^*) in the viscous-elastic region, and at the same time by a G_{mm} value comparable to that of traditional HMA mixtures prepared with high quality natural aggregates.
5. The subsequent rank comparison between the ideal and the reference mix further confirmed what already emerged in the first phase of the research: the S-50 mixture showed excellent Marshall stability and extended fatigue life.

References

[1] P. Ghisellini, C. Cialani, S. Ulgiati, A review on circular economy: The expected transition to a balanced interplay of environmental and economic systems, J. Clean. Prod. 114 (2016) 11-32 https://doi.org/10.1016/j.jclepro.2015.09.007.

[2] L. Devulapall, S. Kothandaraman, G. Sarang, A review on the mechanisms involved in reclaimed asphalt pavement, Int.

J Pavement Res Technol 12 (2) (2019) 185-196 https://doi.org/10.1007/s42947-019-0024-1.

[3] L.D. Poulikakos, C. Papadaskalopoulou, B. Hofko, F. Gschösser, A. Cannone Falchetto, M. Bueno, M. Arraigada, J., Sousa, R. Ruiz, C. Petit, M. Loizidou, M.N. Partl, Harvesting the unexplored potential of European waste materials for road construction, Resour. Conserv. Recy. 116 (2017) 32-44 https://doi.org/10.1016/j.resconrec.2016.09.008.

[4] I. Rodríguez-Fernández, P. Lastra-González, I. Indacoechea-Vega, D. Castro-Fresno, Recyclability potential of asphalt mixes containing reclaimed asphalt pavement and industrial by-products, Constr. Build. Mater. 195 (2019) 148-155. https://doi.org/10.1016/j.conbuildmat.2018.11.069.

[5] P.T. Sherwood, Alternative Materials in Road Construction: A Guide to the Use of Recycled and Secondary Aggregates, Thomas Telford, London, 2001.

[6] P. S. Kandhal, R. B. Mallick, Pavement Recycling Guidelines for State and Local Governments. National Center for Asphalt Technology. Report Number FHWA-SA-98-042. Federal Highway Administration, Washington, DC., 1997.

[7] G. Flores, J. Gallego, F. Giuliani, F. Autelitano, Aging of asphalt binder in hot pavement rehabilitation, Constr. Build. Mater. 187 (2018) 214-219 https://doi.org/10.1016/j.conbuildmat.2018.07.216.

[8] A. Stimilli, A. Virgili, F. Giuliani, F. Canestrari, In plant production of hot recycled mixtures with high reclaimed asphalt pavement content: a performance evaluation, RILEM Bookseries 11 (2016) 927-939 https://doi.org/10.1007/978-94-017-7342-3_74.

[9] M. Stroup-Gardiner, Selection guidelines for in-place recycling projects, Transp. Res. Rec. 2306 (2012) 3-10 https://doi.org/10.3141/2306-01.

[10] M. Bocci, F. Canestrari, A. Grilli, E. Pasquini, D. Lioi, Recycling techniques and environmental issues relating to the widening of a high traffic volume Italian motorway, Int. J. Pavement Res. Technol. 3 (4) (2010) 171-177.

[11] CM-P. Montoliu, R. C. Barrasa, E. G. Bustamante, Generation of circular economy models and use of renewable materials for a more sustainable pavements construction. Carreteras 4 (223) (2019) 62-70.

[12] W. L. Leendertse, M. E. M. Schäffner, S. Kerkhofs, Introducing the circular economy in road construction, Life-Cycle Analysis and Assessment in Civil Engineering: Towards an Integrated Vision - Proceedings of the 6th International Symposium on Life-Cycle Civil Engineering, IALCCE 2018, Ghent, 2019, pp.1639-1644.

[13] WSA, World Steel in Figures 2019. World Steel Association, Brussels, 2019.

[14] BIR, World steel recycling in figure 2011 – 2015. Steel scrap - a raw material for steelmaking. Bureau of International Recycling aisbl, Brussesls, 2016.

[15] C. Shi, Steel slag - its production processing and cementitious properties, J. Mater. Civil Eng. (ASCE) 16 (3) (2004) 230-236 https://doi.org/10.1061/(ASCE)0899-1561(2004)16:3(230).

[16] I.Z. Yildirim, M. Prezzi, Use of Steel Slag in Subgrade Applications. Publication Number FHWA/IN/JTRP-2009/32. Joint Transportation Research Program, Indiana Department of Transportation and Purdue University, West Lafayette, Indiana, 2009.

[17] F. Autelitano, F. Giuliani, Swelling behavior of electric arc furnace aggregates for unbound granular mixtures in road construction, Int. J. Pavement Res. and Technol. 8 (2) (2015) 103-111 https://doi.org/10.6135/ijprt.org.tw/2015.8(2).103.

[18] A. Santamaria, F. Faleschini, G. Giacomello, K., Brunelli, J.-T. San José, C. Pellegrino, M. Pasetto, Dimensional stability of electric arc furnace slag in civil engineering applications, J. Clean. Prod. 205 (2018) 599-609 https://doi.org/10.1016/j.jclepro.2018.09.122.

[19] I.Z. Yildirim, M. Prezzi, Chemical, mineralogical, and morphological properties of steel slag, Adv. Civ. Eng. (2011) .https://doi.org/10.1155/2011/463638.

[20] A. Tossavainen, F. Engstrom, Q. Yang, N. Menad, M. Lidstrom Larsson, B. Bjorkman, Characteristics of steel slag under different cooling conditions, Waste Manage 27 (2007) 1335-1344 https://doi.org/10.1016/j.wasman.2006.08.002.

[21] F. Engström, M. Lidström Larsson, C. Samuelsson, Å. Sandström, R. Robinson, B. Björkman, Leaching behavior of aged steel slags, Steel Res. Int. 85 (4) (2014) 607-615 https://doi.org/10.1002/srin.201300119.

[22] S. Neuhold, A. van Zomeren, J.J. Dijkstra, H.A. van der Sloot, P. Drissen, D. Algermissen, D. Mudersbach, S. Schüler, T. Griessacher, J.C. Raith, R. Pomberger, D. Vollprecht, Investigation of possible leaching control mechanisms for chromium and vanadium in electric arc furnace (EAF) slags using combined experimental and modeling approaches, Minerals 9 (9) (2019) 525 https://doi.org/10.3390/min9090525.

[23] Y. Jiang, T.-C. Ling, C. Shi, S.-Y. Pan, Characteristics of steel slags and their use in cement and concrete-A review. Resour. Conserv. Recy. 136 (2018) 187-197 https://doi.org/10.1016/j.resconrec.2018.04.023.

[24] I. Netinger Grubeša, I. Barišic, A., Fucic, S.S. Bansode, Characteristics and Uses of Steel Slag in Building Construction, Woodhead Publishing, Saewstone, 2016.

[25] G.C. Wang, The Utilization of Slag in Civil Infrastructure Construction, Woodhead Publishing, Duxford, 2016.

[26] H. Yi, G. Xu, H. Cheng, J. Wang, Y. Wan, H. Chen, An overview of utilization of steel slag, Procedia Environ. Sci. 16 (2012) 791-801 https://doi.org/10.1016/j.proenv.2012.10.108.

[27] F. Autelitano, F. Giuliani, Electric arc furnace slags in cement-treated materials for road construction: Mechanical and durability properties, Constr. Build. Mater. 113 (2016) 280-289 https://doi.org/10.1016/j.conbuildmat.2016.03.054.

[28] R.J. Gonawala, R. Kumar, K.A. Chauhan, Usage of crushed EAF slag in granular sub-base layer construction, Adv. Intel. Syst. Comput. 757 (2019) 257-266 https://doi.org/10.1007/978-981-13-1966-2_22.

[29] M. Skaf, J. Manso, Á. Aragón, J. Fuente-Alonso, EAF slag in asphalt mixes: a brief review of its possible re-use. Resourc. Conserv. Recy. 120 (2017) 176-185 https://doi.org/10.1016/j.resconrec.2016.12.009.

[30] H. Wen, S. Wu, S., Bhusal, S, Performance evaluation of asphalt Mixes containing steel slag aggregate as a measure to resist studded tire wear, J. Mater. Civil. Eng. 28 (5) (2016) https://doi.org/10.1061/(ASCE)MT.1943-5533.0001475.

[31] R. Vaiana, F., Balzano, T. Iuele, V. Gallelli, Microtexture performance of EAF slags used as aggregate in asphalt mixes: A comparative study with surface properties of natural stones, Applied Sciences (Switzerland). 9 (15) (2019) https://doi.org/10.1016/10.3390/app9153197.

[32] E.A. Oluwasola, M.R. Hainin, M.M.A. Aziz, Comparative evaluation of dense-graded and gap-graded asphalt mix incorporating electric arc furnace steel slag and copper mine tailings, J. Clean. Prod. 122 (2016) 315-325 https://doi.org/10.1016/j.jclepro.2016.02.051.

[33] M. Pasetto N. Baldo, Experimental evaluation of high performance base course and road base asphalt concrete with electric arc furnace steel slags, J. Hazard. Mater. 181 (2010) 938-948 https://doi.org/10.1016/j.jhazmat.2010.05.104.

[34] M.L. Pattanaik, R. Choudhary, B. Kumar, A. Kumar, Mechanical properties of open graded friction course mixtures with different contents of electric arc furnace steel slag as an alternative aggregate from steel industries, Road Mater. Pavement Des. (2019) https://doi.org/10.1080/14680629.2019.1620120.

[35] M.J. Qazizadeh, H. Farhad, A. Kavussi, A. Sadeghi, Evaluating the fatigue behavior of asphalt mixtures containing electric arc furnace and basic oxygen furnace slags using surface free energy estimation, J. Clean. Prod. 188 (2018) 355-361 https://doi.org/10.1016/j.jclepro.2018.04.035.

[36] S. Sorlini, A. Sanzeni, L. Rondi, Reuse of steel slag in bituminous paving mixtures, J. Hazard. Mater. 209-210 (2012) 84-91 https://doi.org/10.1016/j.jhazmat.2011.12.066.

[37] A. Bonati, S, Rainieri, G. Bochicchio, B. Tessadri, F. Giuliani, Characterization of thermal properties and combustion behaviour of asphalt mixtures in the cone calorimeter. Fire Saf. J. 74 (2015) 215-31 https://doi.org/10.1016/j.firesaf.2015.04.003.

[38] M. Fakhri, A. Ahmadi, Recycling of RAP and steel slag aggregates into the warm mix asphalt: A performance evaluation, Constr. Build. Mater. 147 (2017) 630+-638 https://doi.org/10.1016/j.conbuildmat.2017.04.117.

[39] F.C.G. Martinho, L.G. Picado-Santos, S.D. Capitão, Influence of recycled concrete and steel slag aggregates on warm-mix asphalt properties, Constr. Build. Mater. 185 (2018) 684-696 https://doi.org/10.1016/j.conbuildmat.2018.07.041.

[40] M. Pasetto, N. Baldo, Dissipated energy analysis of four-point bending test on asphalt concretes made with steel slag and RAP, Int. J. Pavement Res. Technol. 10 (5) (2017) 446-453 https://doi.org/10.1016/j.ijprt.2017.07.004.

[41] I.M. Asi, H.Y. Qasrawi, F.I. Shalabi, Use of steel slag aggregate in asphalt concrete mixes, Can. J. Civ. Eng. 34 (8) (2007) 902-911 https://doi.org/10.1139/l07-025.

[42] A. Kavussi, M.J. Qazizadeh, Fatigue characterization of asphalt mixes containing electric arc furnace (EAF) steel slag subjected to long term aging, Constr. Build. Mater. 72 (2014) 158-166 https://doi.org/10.1016/j.conbuildmat.2014.08.052.

[43] M. Shiha, S. El-Badawy, A. Gabr, Modeling and performance evaluation of asphalt mixtures and aggregate bases containing steel slag, Constr. Build. Mater. (2020) https://doi.org/10.1016/j.conbuildmat.2020.118710.

[44] M. Skaf, E. Pasquini, V. Revilla-Cuesta, V. Ortega-López, Performance and durability of porous asphalt mixtures manufactured exclusively with electric steel slags, Materials 12 (20) (2019) 3306 https://doi.org/10.3390/ma12203306.

[45] P. Ahmedzade, B. Sengoz, Evaluation of steel slag coarse aggregate in hot mix asphalt, J. Hazard. Mater. 165 (2009) 300-305 https://doi.org/10.1016/j.jhazmat.2008.09.105.

[46] Q. Li, Y. Qiu, A. Rahman, H. Ding, Application of steel slag powder to enhance the low-temperature fracture properties of asphalt mastic and its corresponding mechanism, J. Clean. Prod. 184 (2018) 21-31 https://doi.org/10.1016/j.jclepro.2018.02.245.

[47] S. Masoudi, S.M. Abtahi, A. Goli, A. Evaluation of electric arc furnace steel slag coarse aggregate in warm mix asphalt subjected to long-term aging, Constr. Build. Mater. 135 (2016) 260-266 https://doi.org/10.1016/j.conbuildmat.2016.12.177.

[48] American Society for Testing and Materials International, Standard Test Method for Dynamic Modulus of Asphalt Mixtures. D3497. ASTM, West Conshohocken, PA, 2003.

[49] American Society for Testing and Materials International, Standard Test Method for Theoretical Maximum Specific Gravity and Density of Asphalt Mixtures. D2041. ASTM, West Conshohocken, PA, 2019.

[50] American Society for Testing and Materials International, Standard Test Method for Bulk Specific Gravity and Density of Non-Absorptive Compacted Asphalt Mixtures. D2726. ASTM, West Conshohocken, PA, 2019.

[51] H. U. Bahia, B. C. Paye, Using the gyratory compactor to measure mechanical stability of asphalt mixtures. Final Report Number WHRP 05-02. Wisconsin Department of Transportation, Madison, WI, 2004.

[52] American Society for Testing and Materials International, Standard Test Method for Marshall Stability and Flow of Asphalt Mixtures. D6927. ASTM, West Conshohocken, PA, 2015.

[53] American Society for Testing and Materials International, Standard Test Method for Indirect Tensile (IDT) Strength of Asphalt Mixtures. D6931. ASTM, West Conshohocken, PA, 2017.

[54] J.M. Read, A.C. Collop, Practical fatigue characterisation of bituminous paving mixtures, J. Assoc. Asphalt Pav. 66 (1997) 74-108.

[55] S.F. Said, Validation of indirect tensile test for fatigue testing of bituminous mixes VTi notat 8. The Swedish National Road and Transport Research Institute, Linköping, 1998.

[56] G.M. Rowe, Performance of asphalt mixtures in the trapezoidal fatigue test (with discussion). J. Assoc. Asphalt Pav. 62 (1993) 344-384.

[57] American Society for Testing and Materials International, Standard Test Method for Effect of Moisture on Asphalt Concrete Paving Mixtures. D4867. ASTM, West Conshohocken, PA, 2014.